Proceedings of the 21st ICSMGE, Vienna, Austria, 14 – 19 June 2026. Pistrol, Adam & Schweiger (eds.)
Published by: ÖGG, Austrian Society for Geomechanics, Salzburg, Austria, ISBN 978-3-9503898-4-5
https://doi.org/10.53243/ICSMGE2026-962

Continuous stiffness monitoring of granular layers of pavements by bender elements

Carolina Briceño, Manuel Parente, Mohammad Roshan, Miguel Azenha, António Gomes Correia
University of Minho, ISISE, ARISE, Department of Civil Engineering, Guimarães, Portugal, id8649@alunos.uminho.pt

João Rocha
CMEMS-UMinho, University of Minho, Guimarães, Portugal

Marcos Martins
INESC TEC, Facultade de Engenharia da Universidade do Porto, Porto, Portugal

Joyce Chidassicua, Ionut Moldovan
Universidade Lusófona, Faculty of Engineering, Lisbon, Portugal.
CERIS, Instituto Superior Técnico, Universidade de Lisboa.

Helder Silva
BUILT CoLAB – Collaborative Laboratory for the Future Built Environment, Porto, Portugal.

Erol Tutumluer,
University of Illinois at Urbana-Champaign, Illinois, USA.

ABSTRACT: The continuous expansion of road networks poses a growing need for advanced geotechnical monitoring solutions that lead to the optimization of road maintenance. Despite the structural importance of unbound granular layers that form the base and subbase of flexible pavements, their continuous monitoring over time has been difficult to perform. To contribute to the development of an effective monitoring system for the dynamic stiffness of granular layers, a numerical and experimental study was carried out to develop an advanced continuous monitoring setup based on bender element sensors, ready to be implemented into pavement infrastructures. Multiple challenges were overcome to develop this monitoring setup, including (i) balancing the need to protect the fragile piezoelectric bender element from the extreme pressures applied during the compaction of the pavement with the need to ensure the unhindered propagation of the shear wave it triggers; (ii) ensuring optimal coupling between the bender elements and the unbound granular layer; and, (iii) enabling the transmitter bender element to induce enough energy into the geomaterial to sense the propagating wave at large distances. To address the first two challenges, the benders were inserted into a protective metallic capsule using a 3D-printed fixation system designed to improve the fixation of the bender to the capsule and the coupling with the surrounding geomaterial. A numerical study was carried out to optimize the shape of the protection capsule, to be wide enough to allow the transmission of the travelling wave while tight enough to ensure bender element protection. The last challenge was addressed by producing oversized bender elements and a customized amplification system. The resulting system was successfully tested into a large compaction box and is being implemented in the field.

KEYWORDS: Bender element sensor, geotechnical monitoring, dynamic stiffness.

1 INTRODUCTION

The unbound granular layers that form the base and subbase of pavements play a crucial role in the structural integrity of roads, as they are responsible for distributing the loads generated by vehicular traffic effectively (Bzówka et al. 2021; Dushmantha et al. 2025; Erlingsson et al. 2017; Gu et al. 2016; Kafle et al. 2024; Rokitowski & Grygierek 2019) and protecting the subgrade from excessive stress. The performance of these layers depends on several factors such as particle size distribution, fines content and moisture, load history, temperature, among others (Lekarp et al. 2000), exhibiting highly non-linear mechanical behavior dependent on time and external loads (Bzówka et al. 2021; Gkyrtis 2023; Jing et al. 2018; Masad & Little 2004; Osman et al. 2024; Zegeye Teshale et al. 2019). This complexity, along with the continuous expansion of road networks, implies a growing need for advanced geotechnical monitoring solutions with greater accuracy, thereby optimizing road maintenance and management.

There are multiple methods for characterizing unbound granular layers (Correia 1999), including laboratory tests (AASHTO T 307 (1999)) and non-destructive in situ tests such as Falling Weight Deflectometer (FWD) and Light Weight Deflectometer (LWD). However, these methods have multiple limitations, including the need for high-quality, unaltered samples, knowledge of actual stress states in the field, and dependence on back-calculation analysis using non-standardized software, which can affect the variability and accuracy of the results (Sangsefidi et al. 2021). Moreover, these techniques are employed on specific points, (i.e., not continuous over distances) and only at a given instant in time/periodic (i.e., not continuous over time).

Bender element (BE) sensors have also been used to trigger shear waves in granular materials (Yoon et al. 2008; Zeng 2006). Byun and Tutumluer (2017) employed BE sensors in granular materials, demonstrating the potential of these sensors for densely graded granular layers under field conditions. Subsequently, Kang et al. (2021) developed wave transducers with BE sensors to assess the long-term stiffness of the unbound granular layers. These studies indicated the effectiveness of using BE sensors in determining the dynamic stiffness of lower pavement layers.

On the other hand, although periodic inspections or data collection are necessary for managing modern road networks, their sporadic nature limits the early identification of deterioration or potential structural problems. Therefore, implementing a continuous monitoring system is necessary. To this end, the INTENT project (INTENT 2025), funded by the Portuguese Science and Technology Foundation, aims to create

an effective system for the dynamic monitoring of granular layers, based on BE sensors. To achieve this, it was necessary to overcome several challenges, including protecting the fragile piezoelectric BE sensor from extreme pressures during pavement compaction while ensuring the shear wave it generates could propagate without obstruction, ensuring optimal coupling between the BE sensors and the unbound granular layer, and enabling the BE transmitter to deliver enough energy into the geomaterial to detect the propagated wave over long distances.

This paper describes the development of a continuous monitoring system for dynamic stiffness in unbound granular layers using BE sensors. First, the design and manufacture of the sensors and amplifiers are described (Sections 2.1 and 2.3), along with the numerical optimization for their implementation in the granular medium (Section 2.2). Subsequently, the system is experimentally validated in the laboratory (Section 3), and the design of the continuous monitoring system (Section 4) intended for field implementation is presented.

2 DESIGN OF THE BENDER ELEMENT SYSTEM

2.1 *Bender element sensors*

BE sensors are piezoelectric transducers designed to generate and detect shear waves propagating through the soil between a transmitting and a receiving BE. In this study, transmitter and receiver are identical in construction, consisting of ceramic PZT (lead zirconate titanate) sheets glued to form a flexible blade structure. The transducers were enclosed in a PLA mould and encapsulated in a polyurethane composite, protecting against moisture and mechanical impact while preserving acoustic coupling and allowing for the flexural motion of the piezoelectric element (see Figure 1). When excited with a single cycle of a sinusoidal voltage, the PZT elements bend laterally, inducing shear deformation in the surrounding soil and generating a shear wave pulse.

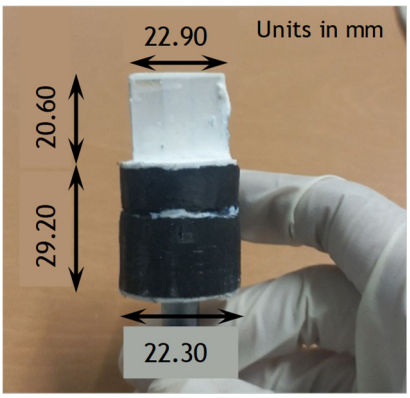

Figure 1: Front view of BE sensor.

2.2 *Numerical optimization of the protection capsule*

Numerical modelling plays a fundamental role in pavement engineering, offering valuable insights into the mechanical behaviour of road structures and embedded sensors under realistic loading conditions. In this study, numerical models enable the simulation of complex interactions between traffic-induced loads and the granular layers of pavements, and endorse the assessment of the performance of BE sensors. The insertion of BE sensors in granular layers of pavements poses critical engineering challenges. On the one hand, BE sensors are very fragile (and expensive) and need protection from the loads applied by the heavy traffic above. For this reason, a decision was made to embed the BE sensors into protective metallic capsules. On the other hand, optimal contact between the BE sensor and the unbound granular material needs to be secured in order to enable the unhindered propagation of the shear wave between transmitter and receiver. The demands of protection and contact are obviously antagonistic, and a well-balanced solution needs to be found.

By employing advanced numerical tools, it is possible to optimize the size of the protection capsule and the insertion depth of the BE sensors. For this purpose, multiple capsule sizes and shapes were essayed, and the best solutions tested in the laboratory. The capsules are based on two stainless steel female T-pipe as shown in Figure 2, with dimensions of 1-1/2 inches and 2 inches. The positioning of the bender element inside the capsule is shown in Figure 3, for the case of the 1-1/2 inches' capsule. The capsules are modelled in their basic form (with no extension) and with three extensions of 8 mm, 15 mm, and 25 mm, screwed to their thread as shown in Figure 3. The question that needs to be answered is which capsule best balances the need for protection with the need for contact between the BE sensor and the surrounding geomaterial.

Because of a lack of space and the fact that the presence of extensions tends to seriously compromise the amplitude of the travelling shear wave, only the results of the capsules without extensions are presented in this paper.

Figure 2: Female T-pipe used in the study.

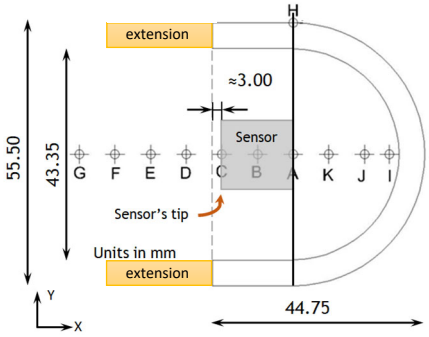

Figure 3: Section 1-1 through the capsule of 1-1/2" with the data points.

Two distinct finite element models are used, namely a quasi-static analysis to evaluate the pressure applied by traffic and an elastodynamic analysis to simulate the propagation of shear waves from the transmitting to the receiving BE sensor. The tests emulate the experimental setup installed the lab and, posteriorly, in the field. Both setups correspond to a bender element located at a depth of 20 cm in the granular base layer, which stands on top of a sub-base layer of 20 cm depth.

Quasi-static analysis. A mobile load passes over a 40 cm thick unbound granular layer with a BE sensor embedded at a 20 cm depth inside the layer. The numerical model is presented in Figure 4. A unit load was applied over a 3 cm length at the top of the granular layer, its position gradually shifted to cover

all of the 100 cm long free surface. The length on which the load is applied is smaller than the typical contact length of a roller compactor, in order to endorse the identification of the most dangerous position it may assume on the surface of the layer. On the lateral and bottom boundaries of the model, normal displacements were fully restricted. The model consisted of 1247 hybrid-Trefftz finite elements, implemented in the FreeHyTE platform (Moldovan et al, 2021).

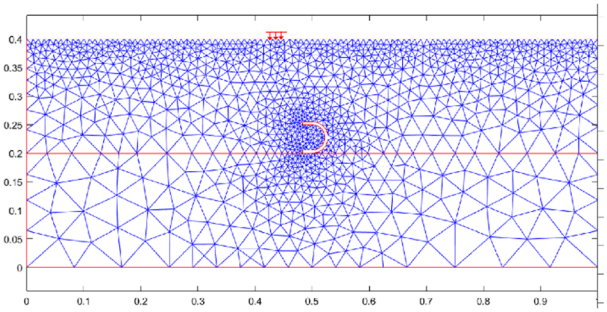

Figure 4: Finite element model of the quasi-static test.

The bender is retracted 3 mm inward from the outer edge of the steel casing, to protect it while ensuring adequate coupling with the granular medium (Figure 4). The resulting stress distribution in the vertical and horizontal directions is evaluated at key points along the capsule (A, B, and C), corresponding to the base, mid-length, and tip of the BE sensor, as well as in its vicinity (points D, E, F, and G).

Figure 5 shows the intensities of the vertical stresses at points A to G for the two sizes of the capsules. The stresses are normalized with respect to the applied vertical load, so their values are given as a percentage of the intensity of the vertical load. This normalization enables the understanding of the stress variation at the selected points. The results show that vertical stress increases from the inside of the capsule towards exterior. At points A and B, the stresses are very similar in both capsules, standing roughly at 0.3% and 0.4% of the applied load. At point C, however, the stress is twice as large for the larger capsule than it is for the capsule with a smaller diameter (1.15% vs 0.60%). This suggests that the 1-1/2" capsule provides better protection of the bender against vertical stress than the 2" capsule. The effectiveness of the capsule is proven by the large discrepancy between the stresses at the last point inside the capsule (point C) and the first point outside (point D). In the latter, the stresses reach roughly 10% of the applied load.

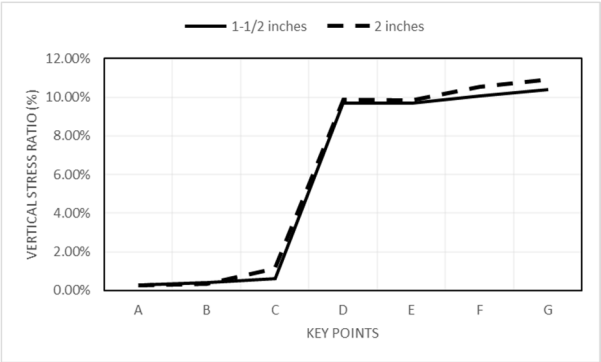

Figure 5: Vertical stress ratio at selected points (% of the applied load).

Elastodynamic analysis. In the elastodynamic model, the geometry and mechanical properties of the transmitter and receiver capsules and the surrounding materials are explicitly included, and absorbing boundary conditions are introduced to eliminate artificial wave reflections.

A distance of 500 mm between the tips of the transmitter and receiver was considered. The model, described in Figure 6, consisted of 3207 hybrid-Trefftz finite elements, implemented in the same FreeHyTE finite element platform as the quasi-static model (Moldovan et al, 2021). The transmitter BE is explicitly modelled, inside the right-hand side capsule. The receiver BE is not explicitly included into the model. The model tracks the amplitude of the lateral displacements associated to the travelling shear wave at different points along the 500 mm propagation trajectory, starting immediately outside the capsule of the transmitter and all the way to the tip of the receiver. Figure 7 shows the lateral displacement ratio (defined as the ratio between the lateral displacement amplitude at the current data point and the lateral displacement amplitude of the tip of the transmitter) in these points, for the two capsule sizes. The displacement ratio at the tip of the transmitter is obviously 100% and not represented in the plots, to improve readability.

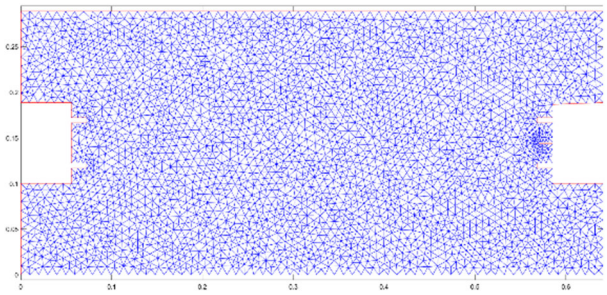

Figure 6: Finite element model of the dynamic test.

For both capsules, the dynamic analysis reveals that the amplitude of the shear wave drastically decreases in the vicinity of the transmitter. Indeed, for both capsules, more than 95% of the signal intensity is lost in the first five centimetres after the tip of the transmitter. The reason for this loss is the cumulated dampening effects of the stiff capsule around the transmitter and of the loose interface material (sand) that fills the capsule of the transmitter. The attenuation is larger in the 1-1/2" capsule because its tighter walls enhance the wave confinement effect.

Moderate attenuation follows as the shear wave travels 500 mm through the unbound granular material. As expected, in this region, the attenuation is independent on the dimension of the capsules, amounting to roughly 3% of the signal's intensity in both cases. Consequently, the displacement signal at the receiver BE only amounts to 1.1% of the initial displacement for the 1-1/2" capsule and 1.7% of the initial displacement for the 2" capsule. This finding supports the need for using amplifiers for transmission and reception BE.

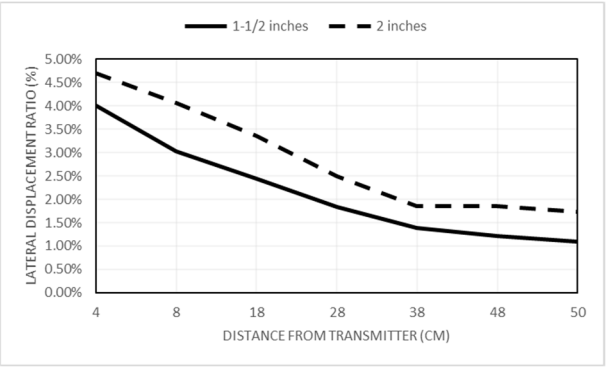

Figure 7: Signal attenuation over distance.

From a practical perspective, it is concluded that the 1-1/2" capsule seems safer to use in the field, as it is much better at protecting the BE sensors. Indeed, the smaller capsule reduces

the stresses applied during compaction to the tip of the BE by a factor of two as compared to the larger capsule. For both capsules, massive attenuation of the waves occurs near the transmitter, so electrical signal amplification is used

2.3 *Design of amplification system*

Two custom electronic amplifiers are designed: a power amplifier to drive a piezoelectric transducer with high-voltage signals (for the emitting sensor), and an instrumentation amplifier to condition the signal received from a second piezoelectric element (for the receiving sensor). The power amplifier is based on a PA96CE operational amplifier, configured with a gain of G = 10 and powered by two ±80 V supply rails. It delivers a high-quality sinusoidal signal to the transmitting BE, enabling a maximum output power of 80 W. The instrumentation amplifier comprises two cascaded LF356N operational amplifiers, powered by galvanically isolated ±5 V regulated supplies. The piezo connects directly to the receiving first stage's amplifier positive terminal, ensuring high input impedance and minimal signal loss. This stage provides a gain of G = 100 and includes a low-pass filter with a cutoff frequency of 530 Hz to remove DC noise components. The second stage offers selectable gain of G = 10 or G = 100 via a jumper and applies a band-pass filter with cutoff frequencies at f_{low} = 530 Hz and f_{high} = 1200 Hz, effectively isolating the target signal at f = 800 Hz. Overall, the instrumentation amplifier achieves a total gain ranging from G = 1000 to G = 10000.

3 EXPERIMENTAL VALIDATION

According to the results provided by the numerical models, the BE sensors were placed inside 1-1/2" diameter stainless steel T-tubes, using plastic 3D-printed holders specially designed to screw into the existent tube threads. Each sensor was placed within a holder with its tip retracted approximately 3 mm from the edge of the protective capsule, leaving about 18 mm of the flexible blade structure unrestrained inside the holder, while the remaining ~2 mm protruded from the holder in contact with the interface material. (Figure 8(a)). This detail was implemented to minimize mechanical interference without affecting the emission or reception of shear waves.

In addition, in order to reinforce the protection of the sensor and ensure optimal coupling between the sensor end and the soil, an additional system was proposed at the end of the tube-holder-sensor assembly. This system consisted of two nylon meshes and an intermediate layer of EN196-1 (CEN, 2016) standardized sand with dimensions of less than 2 mm. The first nylon mesh has an opening that allows the tip of the sensor to be in direct contact with the interface material, preventing sand from entering the support (Figure 8(b)). The second layer was used to stabilize the interface material, consolidating it as a unit (Figure 8(c)).

After preparing the protection system, both sensors (transmitter and receiver) were placed inside a metal box of 80 x 40 x 30 cm³, with each sensor's centre located 10 cm from the base. The T-tubes with the protected sensors were then fixed to vertical stainless-steel rods, and the unbound granular material (UGM), extracted from the site where the sensors will be installed in the field, was placed and compacted in three layers, resulting in a total thickness of 20 cm. It should be noted that a uniform compaction process was applied to all layers of UGM, including the layer above the sensors, as the protection system was expected to ensure the integrity of the sensors adequately under the compaction process used in the laboratory experiments. The particle size distribution of the UGM is shown in Figure 9.

A 25 MHz function generator (TG2511 LX1) was used to generate the excitation signal for the transmitter sensor. A sinusoidal signal in burst mode was selected, with a centre frequency of 800 Hz, an interval between bursts of 50 ms, and an amplitude of 7.4 Vpp. The function generator was connected to the power amplifier, powered by two sources, in order to provide sufficient energy to generate a detectable shear wave in the granular medium. An overview of the setup considered for the experimental validation is shown in Figure 8(d).

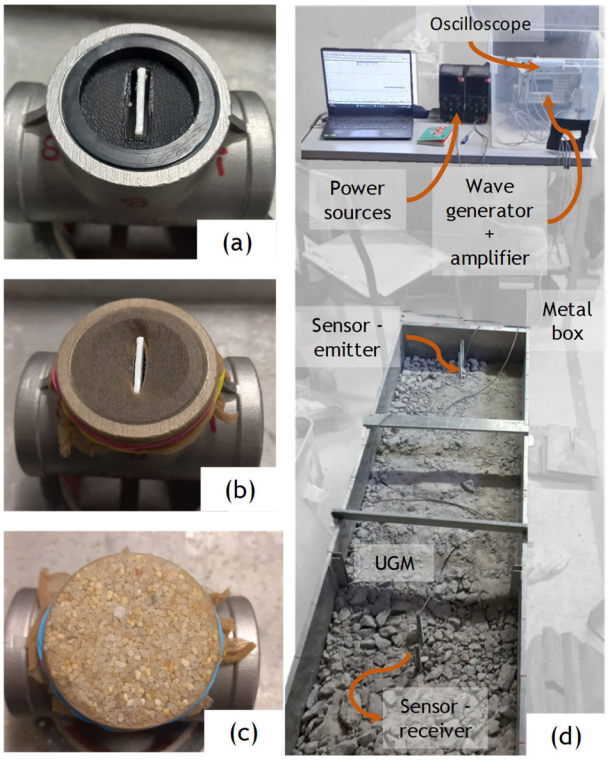

Figure 8: Experimental setup: detail of the protection system for BE sensors consisting of (a) sensor inside the holder and stainless-steel tube, followed by (b) a first nylon mesh with opening, and (c) interface material and outer nylon mesh, and a (d) overview of the laboratory test

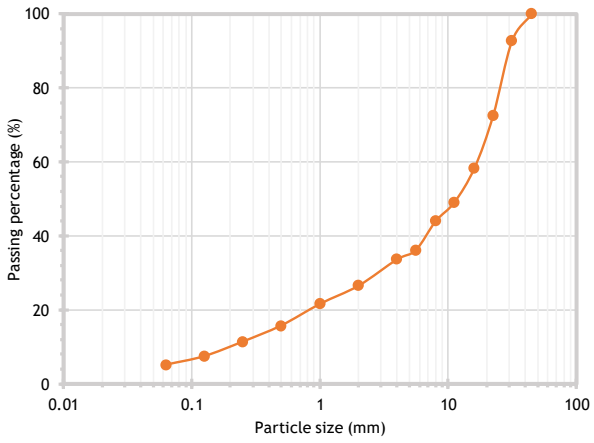

Figure 9: Particle size distribution of the UGM

Several variables were assessed, such as voltage associated with the power amplifier, and distance between sensors. Finally, it was found that for a distance of 76 cm between sensors' tips, it was possible to detect the wave using only the power amplifier, applying a voltage of 80V, obtaining a maximum amplitude of 28.82 µV and a time between emission and reception peaks (Δt) of 8.44 ms, measured using a

PicoScope 4424 digital oscilloscope. Additionally, to improve signal reception, the instrumentation amplifier was incorporated, significantly enhancing the signal and achieving a maximum amplitude of 151.70 mV (See Figure 10).

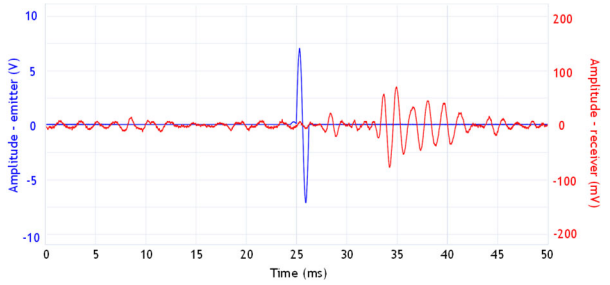

Figure 10: Experimental results at 76 cm between sensors with both amplifiers: emitted (blue) and received (red) waves.

4 MONITORING SYSTEM

The monitoring system for the field installation is designed to perform autonomous and continuous acquisition of multisource data for assessing the mechanical behavior and structural health of unbound granular layers of pavements. It integrates a central application with a set of physical components responsible for signal generation, acquisition, and environmental sensing, optimized for field deployment. The system supports both immediate and scheduled acquisition modes and includes signal filtering, device orchestration, and redundant data storage mechanisms. A schematic diagram of the monitoring system is shown in Figure 11.

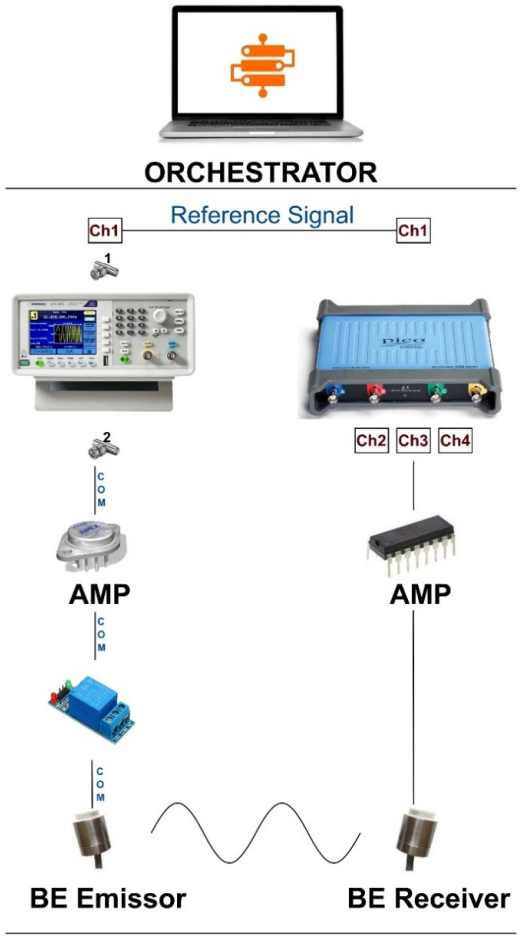

Figure 11: Monitoring system overview.

The core hardware architecture includes a laptop (orchestrator) running the acquisition software, a Tektronix AFG1022 signal generator for producing excitation signals, and a PicoScope 4424A digital oscilloscope for capturing the corresponding waveforms. An Arduino Nano ESP32 microcontroller controls a 16-channel relay board, responsible for switching between BE sensors (transmitters and receivers). The SoilVue10 probe is used for multi-depth soil moisture and temperature measurements, interfaced via a CR350 datalogger. The system also integrates Tapo P100 smart plugs for the remote control of the amplifier. All instruments connect via USB to the main computer through a powered hub, except for the smart plug, which communicates via Wi-Fi.

The software component, developed in Python, includes a modular graphical user interface (Tkinter), device controllers (for generator, oscilloscope, Arduino, datalogger, smart plug), a configuration system (JSON-based), and a robust scheduler (APScheduler). The graphical user interface (GUI) allows real-time control and monitoring of acquisition parameters and device states. Signal acquisition is structured in cycles and stored in a PostgreSQL database (locally and remotely), including metadata such as timestamps, environmental conditions, and filtering status. Filtering is implemented using zero-phase Butterworth filters (4th-order) with configurable low- and high-pass cutoff frequencies, applied to the averaged receiver signal.

The system's architecture emphasizes fault tolerance and automation. It detects and reconnects disconnected devices, verifies data integrity, and logs all operations for traceability. The amplifier's power is managed automatically via the smart plug, ensuring activation only during acquisition cycles, with built-in safety timeouts. SoilVue10 data is collected hourly via UI automation of the PC400 software and stored in a dedicated database.

Designed for long-term field operation, the system combines flexibility, modularity, and scalability. It enables reliable acquisition of wave propagation data, soil conditions, and inertial motion, supporting the continuous health assessment of road infrastructure using embedded BE sensors.

5 CONCLUSIONS

This paper presents the design, optimization, and experimental validation of a measurement and monitoring system for the dynamic evaluation of unbound granular layers using BE sensors. The development of the system includes the construction of BE sensors, mechanical protection systems optimized through numerical simulation, signal amplification systems, and a monitoring system. The three main challenges were successfully addressed: (i) an optimal protection system was proposed that should secure the integrity of the sensor (but hinders the amplitude of the output signal); (ii) efficient coupling between the sensor end and the medium was ensured through the use of an interface material; and (iii) power and instrumentation amplifiers were built to allow the BE sensor to induce sufficient energy in the geomaterial to detect the propagated wave for use in the field under real conditions.

Thus, at the end of the experimental validation, it was observed that for the proposed experimental setup, considering a distance of 76 cm between sensors, an excitation frequency of 800 Hz, and the use of an amplifier for the emission sensor powered by an 80V power source, clear detection of the shear wave was possible. In addition, the implementation of the instrumentation amplifier significantly improved the reception capacity, obtaining a signal amplitude up to 5000 times greater than that obtained with only one amplifier.

Based on these results, the system has demonstrated the robustness necessary to be transferred to the field. Thus, several pairs of protected BE sensors and a continuous monitoring system were installed at selected points in the field for monitoring, which is ongoing and whose results are stored for later analysis. In addition, installation in real conditions allows the system's performance to be evaluated in the face of external loads and environmental conditions. This final phase will validate its performance as a tool for continuous monitoring of dynamic stiffness, verifying whether it performs adequately for practical applications in controlling and monitoring the structural condition of unbound granular layers

6 ACKNOWLEDGEMENTS

This work was financed by Fundação para a Ciência e a Tecnologia (FCT/MCTES) through national funds (PIDDAC) under the R&D Unit *Institute for Sustainability and Innovation in Structural Engineering* (ISISE), reference UIDB/04029/2025, Associate Laboratory *Advanced Production and Intelligent Systems* (ARISE), reference LA/P/0112/2020, and R&D Unit *Civil Engineering Research and Innovation for Sustainability* (CERIS), reference UIDB/04625/2025. Funding was also provided by FCT/MCTES through research project INTENT (2022.06879.PTDC) and PhD scholarship 2023.03777.BD attributed to the third author.

7 REFERENCES

AASHTO T307,1999. *AASHTO T307 - Determining the Resilient Modulus of Soils and Aggregate Materials*. Washington DC.: AASHTO.

Byun, Y.-H., and Tutumluer, E. 2017. Bender elements successfully quantified stiffness enhancement provided by geogrid–aggregate interlock, *Transportation Research Record* 2656(1), 31–39.

Bzówka, J., Grygierek, M., and Rokitowski, P. 2021. Experimental investigation using distributed optical fiber sensor measurements in unbound granular layers, *Engineering Structures* 231, 111767.

Climent, N., Moldovan, I., Correia, A.G. 2022. FreeHyTE: A Hybrid-Trefftz Finite Element Platform for Poroelastodynamic Problems. In *Advances in Transportation Geotechnics IV. Lecture Notes in Civil Engineering*, 164.

Correia, A. G. 1999. Unbound Granular Materials: laboratory testing, in-situ testing and modelling (Editor: A. Gomes Correia). In *Proceedings of an international workshop on modelling and advanced testing for unbound granular materials*, Lisbon, 21-22.

Dushmantha, A., Jayakody, S., Gui, Y., and Gallage, C. 2025. A comprehensive review of the resilient behaviour of unbound granular pavement materials, *Journal of Traffic and Transportation Engineering* 12(3), 522–550.

Erlingsson, S., Rahman, S. and Salour, F. 2017. Characteristic of unbound granular materials and subgrades based on multi stage RLT testing, *Transportation Geotechnics* 13, 28–42.

European Committee for Standardization (CEN), 2016. *EN 196-1: 2016- Methods of Testing Cement. Determination of Strength*. Brussels.

Gkyrtis, K. 2023. Pavement Analysis with the Consideration of Unbound Granular Material Nonlinearity, *Designs* 7(6), 142.

Gu, F., Luo, X., Zhang, Y., Lytton, R., and Sahin, H. (2016) Modeling of unsaturated granular materials in flexible pavements, *E3S Web of Conferences*, 20002.

INTENT, 2025. *Intelligent health monitoring of road pavements*. [online] Available at: https://intent.ulusofona.pt/ [Accessed 8 August 2025]

Jing, P., Nowamooz, H., and Chazallon, C. 2018. Permanent deformation behaviour of a granular material used in low-traffic pavements, *Road Materials and Pavement Design* 19(2), 289–314.

Kafle, B., Baghbani, A., Pempeit, R., and Shrestha, K. 2024. Investigating the Mechanical Behaviour of Unbound Granular Material (UGM) for Road Pavement Construction Applications: A Western Victoria Case Study, *International Journal of Geosynthetics and Ground Engineering* 10(2), 29.

Kang, M., Qamhia, I.I.A., Tutumluer, E., Hong, W-T., and Tingle J.S. 2021. Bender element field sensor for the measurement of pavement base and subbase stiffness characteristics, *Transportation research record* 2675(8), 394–407.

Lekarp, F., Isacsson, U. and Dawson, A. 2000. State of the art. I: Resilient response of unbound aggregates, *Journal of transportation engineering* 126(1), 66–75.

Masad, S. A. and Little, D. N. 2004. *Sensitivity analysis of flexible pavement response and AASHTO 2002 design guide to properties of unbound layers*, Washington.

Moldovan, I.D., Climent, N., Bendea, E.D., Cismasiu, I., Gomes Correia, A. 2021. A hybrid-Trefftz finite element platform for solid and porous elastodynamics, *Engineering Analysis with Boundary Elements*, 124, 155-173

Osman, H., Rodzey, M. Z. I. M., Hasan, M. R. M., Wong, T. L. X., Ghazali, M. F. H. M., Zakaria, Z., and Jameel, M. 2024. Review of bonding behavior, mechanisms, and characterization approach in bituminous materials under different conditions, *Journal of Traffic and Transportation Engineering* 11(6), 1291–1316.

Rokitowski, P. and Grygierek, M. 2019. Initial research on mechanical response of unbound granular material under static load with various moisture content. *Proc. IOP Conference Series: Materials Science and Engineering*. 32040.

Sangsefidi, E., Larkin, T. J. and Wilson, D. J. 2021. The effect of weathering on the engineering properties of laboratory compacted unbound granular materials (UGMs), *Construction and Building Materials*. 276, 122242.

Yoon, H-K., Lee, J-S., Kim, Y-U., and Yoon, S. 2008. Fork blade-type field velocity probe for measuring shear waves, *Modern Physics Letters B*. 22(11), 965–969.

Zegeye Teshale, E., Shongtao, D. and Walubita, L. F. 2019. Evaluation of unbound aggregate base layers using moisture monitoring data, *Transportation Research Record* 2673(3), 399–409.

Zeng, X. 2006. Applications of piezoelectric sensors in geotechnical engineering, *Smart structures and systems* 2(3), 237–251.